ELSEVIER

Thermochimica Acta 266 (1995) 49–64

thermochimica acta

# Extrinsic and intrinsic size effects on the phase transformation and metastability of a glassy crystal ☆

M. Descamps [a], J.F. Willart [a], O. Delcourt [a], M. Bertault [b]

[a] *Lab. de Dynamique et Structure des Matériaux Moléculaires, U.A. CNRS 801, Université de Lille 1, Bât. P5, 59655 Villeneuve d'Ascq, France*

[b] *Groupe Matière Condensée et Matériaux, U.A. CNRS 804, Université de Rennes 1, 35042 Rennes, France*

**Abstract**

The facility offered by disordered glassy crystals to study their ordering phase transformation in real time is used to discuss two unusual finite size effects. The first is the change in the overall transformation kinetics observed when the crystal size competes with a length scale characteristic of a nucleation and growth process. It is shown that this can be used to determine the nucleation rate and the critical size at any temperature. The second is a transient reversion of the order detected in the glass transition temperature range by which the transforming system goes back to its metastable disordered state. It is shown how this phenomenon is correlated with the size of the nuclei produced during a sub-$T_g$ annealing.

*Keywords:* Glassy crystal; Metastable; Phase transformation; Size effect

## 1. Introduction

A first-order phase transition is associated with the possibility of phase coexistence. With an abrupt change in external parameters (temperature, pressure, field), one can bypass the equilibrium transition point and thus place a substance in a metastable situation. Its decay to the stable state involves the formation of localized heterophase fluctuations having the order parameter of the most stable phase. These nuclei grow until they ultimately overgrow the whole sample. Here we are concerned with the kinetics of this transformation and more specifically with manifestations of size

☆ Dedicated to Hiroshi Suga on the Occasion of his 65th Birthday.


*SSDI* 0040-6031(95)02454-9

influence on the behaviour of the undercooled sample. This will lead us to discuss two very different aspects of size effects:

1. The first concerns the modifications of the transformation kinetics of a compound placed in a situation of constrained geometry. They basically involve the competition between the dimension of the system and the average distance $\xi$ between the hetero-phase clusters at the end of the transformation. $\xi(T)$ is a temperature-dependent natural length scale of the undercooled material which is derived from a combination of the nucleation ($N$) and growth ($G$) rates. When the sample size $L$ crosses this characteristic value, a drastic change is expected both in the form of the law of overall transformation kinetics and the value of the relaxation times. Consequently, varying the sample size offers, in principle, a chance to get an assessment of $N$ from overall transformation measurements alone.
2. The second results from the small size of the nuclei in which the transformation initially arises. We shall show that this size reduction can induce stability inversions which depend on the previous thermal history of the sample and on the dynamic parameters with which the experiments are performed.

We shall take as an illustration results obtained from an investigation of "glassy crystals" according to the terminology of Suga and co-workers [1, 2]. These are molecular compounds which show, at high temperature, a crystalline phase with a dynamic orientational disorder of the molecules on their lattice site. In some cases, in particular when the steric hindrance to molecular rotation is high, these so-called "plastic phases" [3] can be strongly undercooled in order to avoid the first-order transition associated with the orientational ordering. Upon rapid and low enough cooling, one observes the manifestation of a conventional glassy state (similar to that obtained when quenching a liquid), namely the heat capacity jump at $T_g$, and a Vogel–Fülcher behaviour of the dynamics. However, the glass transition proceeds from a crystalline phase and the associated freezing is, a priori, mainly that of the large-amplitude rotational motions of the molecules. Such compounds are considered as model systems to study the glass transition [4, 5]. The Osaka group has shown that the possibility observed in "glassy crystals" to freeze only a limited number of degrees of freedom is frequently observed in condensed matter and thus demonstrated that the conventional concept of glass transition can be broadened to mesophases in general.

Because of their low molecular mobility and slowness of transformation, "glassy-crystals" also offer a very favourable situation to investigate the metastable state and the first-order kinetics of transformation upon either shallow or deep quenches.

The possibility of undercooling and quenching *single crystals* of the plastic phase without damage is exploited in order to follow the transformation in real time with X-ray diffraction techniques. This type of study, performed jointly with a thermal analysis, provides a good picture of the microscopic mechanisms which come into play. Analysis of diffractograms in their entirety, as well as analysis of line shapes, enables us to characterize both the order which spreads out in a system and its spatial extension.

The system we have studied is a mixed compound of cyanoadamantane (CNa) and chloroadamantane (Cla): $(CNa)_{1-x}(Cla)_x$ with $x = 0.25$ [5].

A schematic diagram of the Gibbs energy of the compound is illustrated in Fig. 1, allowing the various experiments which are discribed below to be located. Phases I, III and IV respectively correspond to the plastic phase (face-centred cubic Fm3m), the ordered stable phase at low temperature (monoclinic $P2_1/c$) [5] and a metastable phase [6] (probably tetragonal). Upon cooling of phase I, the two transitions (IV–I) and (III–I) are bypassed and the Gibbs diagram could only be established after appropriate long ageing treatments at low temperature. Some of these kinetic investigations will be used to illustrate the size effects discussed below.

When the plastic phase I is undercooled deeply enough, the calorimetric glassy crystal transition is seen at about $T_g = 163$ K where it is signalled by a pronounced jump in the heat capacity and the thermal expansion coefficient [7] (Fig. 2). On crossing the glass transition, no change of the f.c.c. structure typical of phase I can be noticed. The rotational disorder of this phase thus persists but becomes almost static at low temperature.

## 2. Influence of the sample size on the kinetics of phase transformation

### 2.1. Description of one experiment

The study of the transformation I → III after a rather shallow quench reveals the effects of the sample size on the kinetics of a first-order transition. We focus on the time evolution of the fraction of converted sample $X(t)$. Using a time-resolved X-ray diffraction technique, its value is given by

$$X(t) = \frac{I(t) - I(o)}{I(\infty) - I(o)} \tag{1}$$

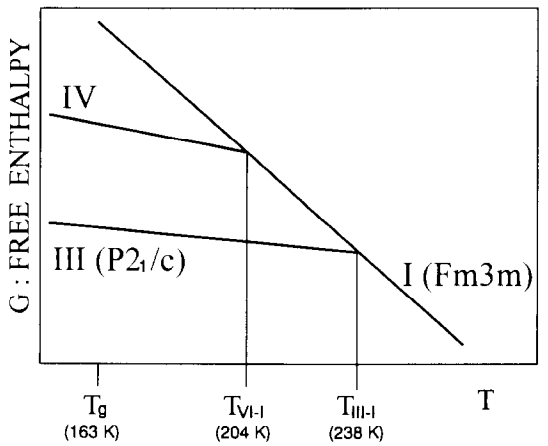


Fig. 1. Schematic diagram of the Gibbs energy of $(CNa)_{0.75}(Cla)_{0.25}$.

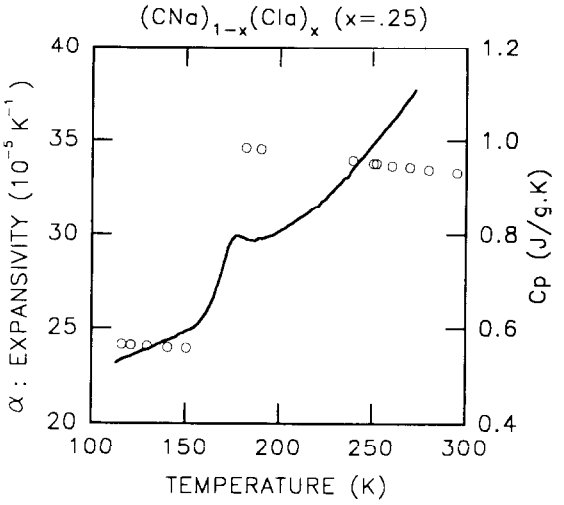


Fig. 2. Thermal expansion coefficient $\alpha$ and $C_p$ curve for $(CNa)_{0.75}(Cla)_{0.25}$ ($\dot{T} = 10$ K min$^{-1}$).

where $I(t)$ is the value at time $t$ of the integrated X-ray intensity of a Bragg peak characteristic of the new emerging phase. Isothermal growth curves, $X(t)$, for $(CNa)_{0.75}(Cla)_{0.25}$ have been obtained at different temperatures between 204 and 238 K where phases III and I can only coexist in a metastable equilibrium, and for each temperature, with samples of various sizes, from a single crystal (with dimensions $0.8 \times 0.8 \times 0.8$ mm) to fine powder ($\approx 10$ μm) obtained by grinding.

The main results are as follows [8]. On a macroscopic sample, $X(t)$ is sigmoidal, whatever the temperature. While the half-completion times, $t_{1/2}$, are very dependent on the transformation temperature (Fig. 3(a)), all the growth curves can be fairly well scaled onto a single S-shaped master curve when plotted as a function of $t/t_{1/2}$ (Fig. 3(b)). At a given temperature, decreasing the grain size induces a lengthening of the kinetics (Fig. 4). This shows the predominant influence of the sample size over the effect of increased heterogeneous nucleation rate, which may be expected after grinding. One may, moreover, notice that the shape of the growth curve evolves with sample size, changing from sigmoidal to near-exponential behaviour when the sample becomes more and more subdivided. As a result, the different growth curves no longer fall on a single universal curve when they are plotted against the reduced time $t/t_{1/2}$ (inset of Fig. 4).

### 2.2. *Dimensional analysis of a transformation law*

#### 2.2.1. *Classical nucleation-and-growth picture*

Homogeneous nucleation is a thermally activated process by which some droplets have to be formed in order to enable the phase transformation to occur. In the conventional Becker–Döring capillarity theory [9], the formation free energy ($\varepsilon$) of

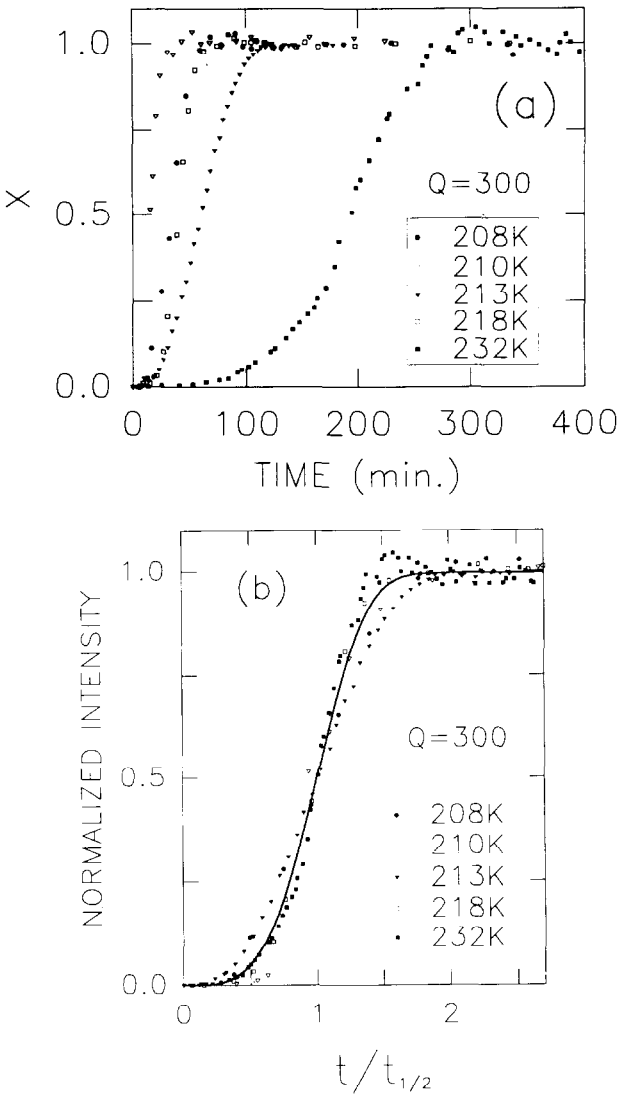


Fig. 3. (a) Time evolutions of the transformed fraction $X(t)$ after quenching single crystals (in phase I) at different temperatures in the domain of stability of phase III (see Fig. 1). (b) Previous growth curves scaled by plotting $X$ vs. $t/t_{1/2}$ where $t_{1/2}$ is the half-completion time. They are well represented by a single Avrami law with $d = 3$.

a droplet is assumed to result from the competition between an unfavourable positive surface free energy and a negative bulk energy. Surface energy prevails for small droplets. The latter thus have a good chance of growing if they exceed a certain critical size $r^*(T)$ and overcome the nucleation barrier $\varepsilon^*(T)$. Nucleation

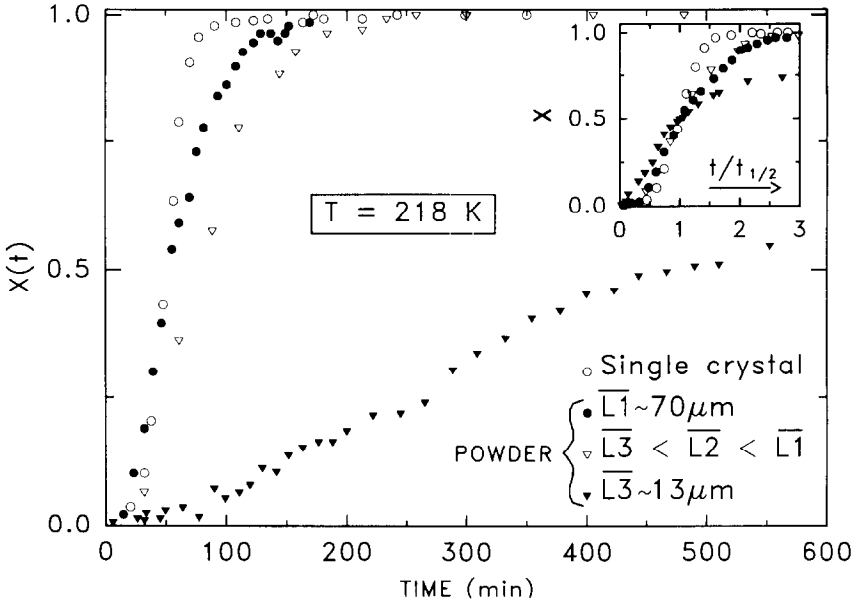


Fig. 4. Time dependence of the transformed fraction at 218 K of the converted sample $X(t)$, for a single crystal and several powder samples of $(CNa)_{0.75}$ $(Cla)_{0.25}$ with different mean grain sizes. The inset shows that these curves cannot be superimposed on a single master curve by rescaling the time.

events thus occur at a steady rate

$$N(T) = f_0(T) \exp\left(\frac{-\varepsilon^*}{kT}\right) \tag{2}$$

where $f_0$ is an "attempt frequency" for the addition of particles to the stable phase across the interface. If one assumes that the driving force $\Delta F$ is proportional to the undercooling $\Delta T$ then $r^* \sim 1/\Delta T$ and $\varepsilon^* \sim 1/\Delta T^2$. Once a stable nucleus is formed it will continue to grow during isothermal annealing at a linear rate which, for an interface-controlled process, is given by the Turnbull [10] semi-phenomenological expression

$$G(T) = G_0(T)\left(1 - \exp\left(\frac{-\Delta F}{kT}\right)\right) \tag{3}$$

where $G_0$ is expected to have an Arrhenius temperature behaviour.

*2.2.2. Natural length scale for overall transformation kinetics*

The global transformation, observed through $X(t)$, and as a consequence the effectively accessible undercooling, are strongly sensitive to the combined effects of both nucleation and growth.

From the simple dimensional analysis [11] of a 3-dimensional nucleation (at rate $[N] = L^{-3}t^{-1}$) and growth (at linear rate $[G] = Lt^{-1}$) transformation, a natural length scale

$$\xi = (G/N)^{1/4} \tag{4}$$

and a natural time scale

$$t_a = (NG^3)^{-1/4} \tag{5}$$

arise.

The competition between $\xi$ and the real macroscopic size $L$ of the system induces a change in kinetic regime as discussed in Ref. [8] and is sketched in Fig. 5.

In the limiting cases of the very large and very small sample sizes, one expects the following two kinetic growth laws for the transformed fraction $X(t)$.

(i) If $L \gg \xi$, we must take into account at the same time the progressive decrease in nucleation efficiency and the impingement of neighbouring grains at the end of the transformation. At the thermodynamic limit, this leads to the well-known Avrami law

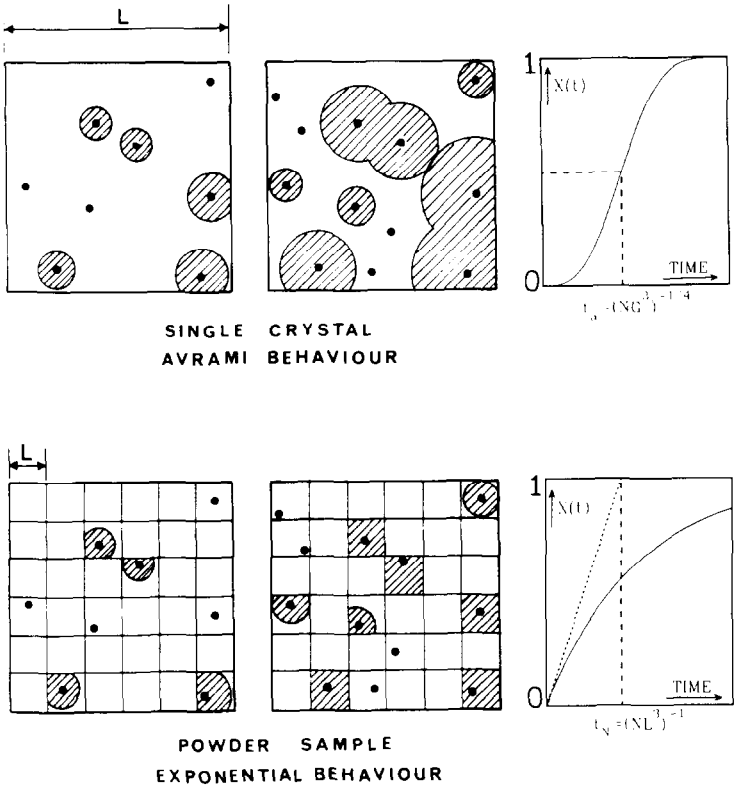


Fig. 5. Overall transformation kinetics. Illustration of the crossover from Avrami ($L \gg \xi$) to nucleation ($L \ll \xi$) regime.

which, in 3 dimensions, is given by

$$X(t) = 1 - \exp\left(-\frac{4\pi}{3}\left(\frac{t}{t_a}\right)^4\right) \tag{6}$$

This is a universal sigmoidal function of the size-independent time scale $t_a$.

(ii) If $L \ll \xi$, each cell is immediately converted once nucleated and the transformed fraction coincides with the fraction of nucleated cells. For cells of linear size $L$, it is calculated by

$$\frac{dX}{dt} = (1 - X)L^3 N \Rightarrow X(t) = 1 - \exp\left(-\frac{t}{t_N}\right) \tag{7}$$

where the characteristic time $t_N = (L^3 N)^{-1}$ is now highly size-dependent.

Fig. 6 shows the results of a numerical simulation of the changes with the grain size $L$ of the $X(t)$ function for assumed fixed values of $N$ and $G$ (and so, for fixed values of

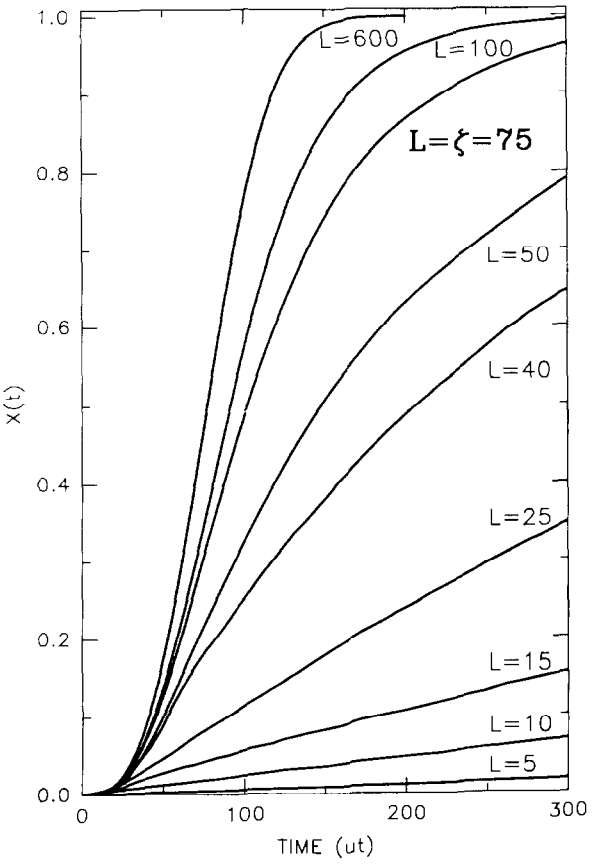


Fig. 6. 2-Dimensional simulation of the time evolution of the transformed fraction $X(t)$ for different grain sizes but fixed values of the nucleation and growth rates corresponding to $\xi = 75$ and $t_a = 75$.

$\xi$ and $t_a$). The change in kinetic regime and associated scaling laws are discussed more deeply in Ref. [8].

In the course of sample size reduction, by grinding or confinement, one may expect a change in the nucleation parameters which have previously been assumed to be an intrinsic characteristic of the sample at a given temperature. The described size competition is, however, certainly one of the mechanisms which allows an expansion of the apparent metastable domain by size reduction when nucleation and growth both occur.

### 2.3. *Consistency of experimental results and estimation of transformation parameters*

Analysis of the size modification effects given in Section 2.2 clarifies the experiments described in Section 2.1. The kinetic investigations performed on a single crystal certainly correspond to a situation which is close to the thermodynamic limit ($L \gg \xi$). In particular, the validity of Avrami scaling law in this situation is demonstrated by the experimental curves shown in Fig. 3. By comparing the experimental size reduction effects as shown in Fig. 4 to the simulation results seen in Fig. 6 one can understand that the kinetic regime changes drastically when the sample size crosses the natural length scale $\xi$ involved in the nucleation and growth process at the considered temperature. One can therefore estimate $\xi$ to be a few tens of μm at 218 K. From Eqs. (5) and (7), the measured values of the characteristic times $t_a$ and $t_N$ corresponding respectively to the situations where we expect $L \gg \xi$ and $L \ll \xi$, then allow estimation of both the nucleation and growth rates $N$ and $G$. From the results at 218 K (Fig. 4), one obtains

$$t_a \sim 1800\,\text{s and } t_N \sim 6 \times 10^4\,\text{s (for } \bar{L}_3 \sim 13\ \mu\text{m)} \tag{8}$$

which gives

$$N \sim 10^{10}\,\text{m}^{-3}\,\text{s}^{-1} \text{ and } G \sim 200\ \text{Å s}^{-1} \tag{9}$$

A test of the consistency of the analysis is supplied by the calculation of $\xi = (G/N)^{1/4} \sim 40$ μm which is in good agreement with what is expected from a mere inspection of the change in regime shown in Fig. 4.

This analysis shows that a controlled size reduction may provide an interesting tool to estimate $N$ and $G$ by measuring only the overall transformation kinetics but in various regimes. If we have a good order of magnitude estimate of $N$ at one given temperature, we can then evaluate its temperature dependence as well as that of the critical radius $r^*(T)$ by assuming that classical homogeneous steady nucleation theory is applicable through an adaptation of the Turnbull–Fisher [9] absolute reaction rate theory to the plastic-to-brittle phase transition. It is then only required to know the latent heat of transformation and the temperature dependence of the molecular reorientational process occurring at the interface which presumably dominates the "attempt frequency" term $f_0$. Using dielectric spectroscopy data [12] this yields the results shown in Fig. 7.

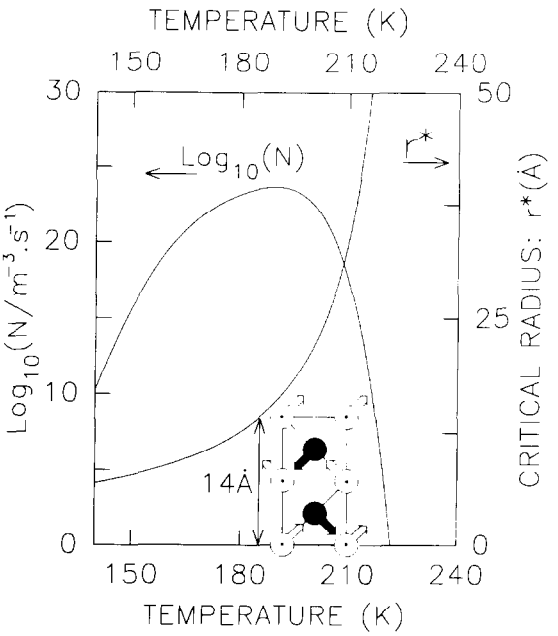


Fig. 7. Temperature evolutions of the nucleation rate ($N$) and the critical radius for nucleation ($r^*$) for the transformation I → III. These evolutions have been determined from the stationary nucleation rate estimated at 218 K by the analysis of the size reduction effects (see text) and in the framework of the classical homogeneous nucleation theory [9]. The inset shows the size of the cell in phase III. Note that the critical radius for phase III rapidly becomes smaller than the lattice parameter for deep undercooling.

These evaluations are made within the bounds of classical theories. To the extent that it is applicable at high super-cooling, one may notice that the expected size of the critical nucleus would be extremely small (< 10 Å) as $T$ approaches $T_g$. It is certainly unphysical to conceive well-defined clusters of such a small size. However this stresses the fact that very small characteristic lengths are certainly involved in the transformation processes occurring near $T_g$. This point is of importance with regard to the size effects invoked afterwards.

## 3. Stability inversion

The temperature evolution of the nucleation rate of phase III from phase I, illustrated in Fig. 7, is only virtual at low temperature. In fact, when the plastic phase is annealed below ~ 200 K, the first product of the transformation is phase IV and much longer annealing times are necessary to obtain phase III. These two phases have been identified by X-ray diffraction and the imbricated kinetics of the transformation I → IV → III are described elsewhere [6]. The investigation of the phase transitions involved between the different phases after various annealing times led us to propose

that phase IV is metastable with regard to III, according to the Gibbs diagram shown in Fig. 1.

We present here a brief account of experiments performed after deep quenches of phase I near the calorimetric glass transition temperature $T_g$.

We have studied the effect of isothermal annealing at different temperatures $T_a$ for annealing times $\Delta t_a$ varying from a few minutes to several hours. The influence of these thermal treatments on the $C_p$ curves upon heating have been observed by DSC. The evolutions of the X-ray diffraction spectra of quenched single crystals have been followed in real time during similar annealing and subsequent reheating.

### 3.1. DSC signature of the relaxation

The obtained $C_p$ curves are presented in Fig. 8; the main features are:

(i) The jump in the heat capacity which signals the kinetic glass transition of the crystal at $T_g$ (see also Fig. 2). This occurs when the rate of the slowest

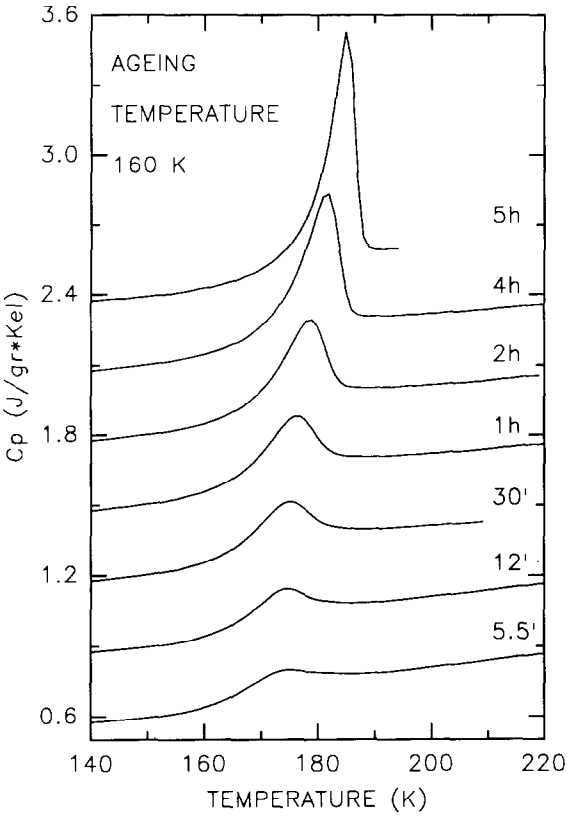


Fig. 8. $C_p$ curves obtained upon heating ($\dot{T} = +10\,\mathrm{K\,min^{-1}}$) after different annealing times at $T_a = 160\,\mathrm{K}$. For clarity, each curve has been shifted 0.3 $\mathrm{J\,g^{-1}\,K^{-1}}$ above the one below, the left-hand axis corresponding to the bottom curve.

molecular reorientations becomes commensurate with the rate of change of temperature: $\dot{T}$.

(ii) An endothermic peak just above $T_g$ which develops as the annealing time increases. Comparing the different curves, we may notice that the peak maximum shifts towards high temperatures as $\Delta t_a$ increases.

The $C_p$ peak looks very much like the overshoot classically observed during the reheating of annealed conventional glasses. Furthermore, it evolves in the expected way with annealing time. This overshoot is commonly interpreted as being a consequence of the structural relaxation of the glass towards the metastable liquid state in internal equilibrium. The heat capacity maximum thus corresponds to the sample sharply regaining, upon heating, the increase in enthalpy lost during annealing. The retarded return to the metastable state occurs at a temperature where the relaxations become rapid enough. Phenomenologically, the structural state of an annealed glass is measured by a fictive temperature $T_f$ which is defined as that at which the equilibrium liquid has the same enthalpy as the annealed glass. The lower limiting value of $T_f$ is thus the annealing temperature itself in case the glass relaxes towards the equilibrium liquid. Experimentally, the fictive temperature corresponding to one given annealing time is derived from the corresponding $C_p(T)$ curve by a simple equal-area rule [13] based on the extrapolation of the heat capacities measured, respectively, below and above the glass transition region. From the $C_p(T)$ curve of Fig. 9(c) which was obtained after annealing the glassy crystal for 4 h at 160 K, we derive a fictive temperature $T_f \sim 142$ K.

After such a short annealing period, $T_f$ is thus distinctly lower than $T_a$. Therefore, during the annealing the enthalpy of the system has gone beyond the relaxation level which would correspond to a hypothetical equilibrium metastable plastic crystal.

The sizeable endothermic peak cannot thus be only explained by the classical argument of a retarded reequilibration of the metastable plastic phase, i.e. the reequilibration of a homogeneous short-range order (SRO). It thus appears that the relaxing glassy crystal has moved towards a more stable state, and that the reheating leads to a reversion of this order.

### 3.2. *X-ray signature of the relaxation*

Real-time X-ray diffraction experiments performed isothermally after the quench below $T_g$ of a single crystal offer the possibility of following directly the structural relaxation in the reciprocal space [7] of the crystal. A slow evolution of the X-ray pattern appears through the growth of superstructure peaks situated at the X-boundary points of the Brillouin zone which are forbidden reflections of the f.c.c. lattice of phase I. Such peaks reveal a molecular orientational ordering similar to that of phase IV [6].

There is a question about the nature of the associated fluctuations: either they are a short-range order (SRO) which spreads homogeneously in metastable phase I, or they are heterophases (clusters of phase IV ordered internally). This point can be clarified by a careful analysis of the kinetics of the process. As seen on the isothermal evolution of the peak intensity measured at the $\vec{Q} = 121$ position (Figs. 9(a) and 10), the growth after

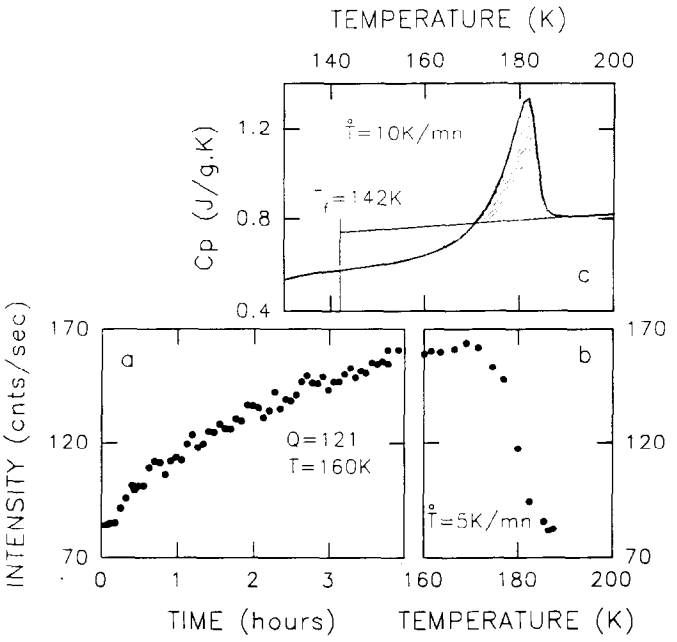


Fig. 9. Evidence of thermal history effects seen through real-time X-ray experiments and thermal analysis of the mixed compound ($x = 0.25$). (a) Temporal evolution of the 121 X-ray superstructure peak after a quench at 160 K. (b) Temperature evolution ($\dot{T} = +5$ K min$^{-1}$) of the peak intensity of the 121 superstructure peak developed during the previous 4-h ageing displayed in (a). (c) DSC curve obtained upon heating ($\dot{T} = +10$ K min$^{-1}$) and after a 4-h ageing at 160 K. The fictive temperature ($T_f = 142$ K) is found to be much lower than the ageing temperature.

quench at $T_a = 160$ K is immediate but it gradually slows down so that saturation is not reached after 8 days. At a temperature so close to the thermodynamic glass transition, it takes much longer than the time required to re-equilibrate totally the glassy phase in its metastable state. This is thus a strong indication that the observed relaxation is not merely that of the short-range structural reorganization towards the metastable state whose freezing is detected at $T_g$ on the experimental time scale. This is confirmed by the analysis of the shape of the peak which is the Fourier transform $S(\vec{Q})$ of the orientational correlation function of the molecules. After a long enough annealing $S(\vec{Q})$ is very close to a Gaussian which is consistent with a mechanism of long-range ordering in heterophase nuclei bounded by interfaces. The coherence length linked to these ordered zones is the inverse of the peak width $\Delta Q^{-1}$ (found to be only 2–3 unit cell sizes after 8 days).

### 3.3. *Order reversion*

When the crystal is reheated after a low-temperature annealing, a rapid collapse of the superstructure peak is observed at the exact temperature of the $C_p$ endothermic

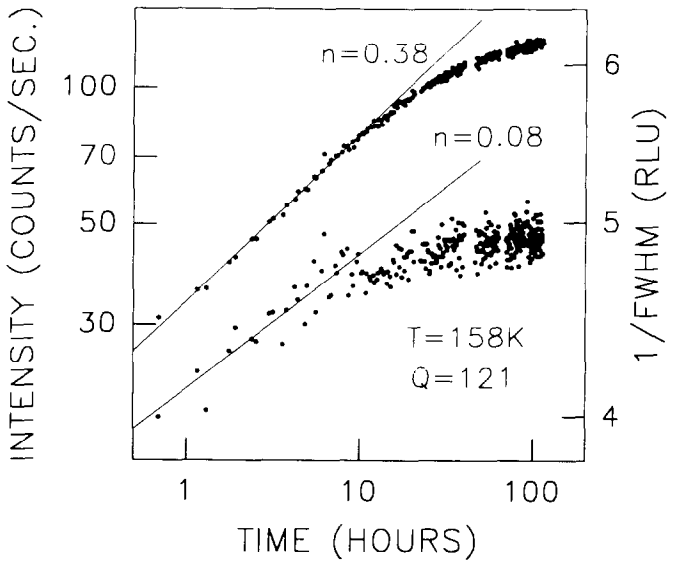


Fig. 10. Log–log plot of the temporal evolution of the X-ray peak intensity and the inverse peak width at the $\vec{Q} = 121$ position in the mixed compound ($x = 0.25$). The straight lines correspond to the steepest tangents whose slopes are respectively $n = 0.38$ and $n = 0.08$.

overshoot obtained after the same thermal history and with a similar heating rate (Fig. 9(b) and (c)). We thus observe a reversion of domains of phase IV and a return to the metastable state I. This occurs at temperatures much lower than the equilibrium transition temperature (found to be $T_{IV-I} \sim 204$ K [6]). The recovery of the metastable phase I does not correspond to a phase transition because it is a transient phenomenon. A new annealing at a higher temperature leads to a new growth of the X-ray superstructure peaks at the same $\vec{Q}$ position and thus a new development of phase IV.

The DSC and X-ray investigation show that the reversion temperature increases when the annealing time $\Delta t_a$ at a given temperature $T_a$ increases. Moreover, Fig. 10 shows a slow sharpening of the superstructure peaks during isothermal annealing. Such a behaviour corresponds to a slow growth of the domain size of the new phase. It thus appears that there is a correlation between the reversion temperature and the size of the domains which vanish. It is not clear at the moment if the finite size effect is attributed to an equilibrium or kinetic phenomena. However the most simple interpretation can be based on the classical nucleation theory (see Section 2.2.1). The reversion could result from a kinetic competition between the sweeping temperature rate and the ability of the nuclei of phase IV to reach new critical size $r^*$ at a new temperature. If the heating rate is high enough the nuclei become unstable and "dissolve" at a temperature where the critical radius becomes higher than their size.

This situation can only be conceived if the growth of the nuclei is low enough. Such a slow growth is shown in Fig. 10 where it also appears that the growth law itself is

unusually weakly time-dependent. In addition to a low molecular mobility effect expected near $T_g$, the growth law reveals a strong decline in cluster development.

## 4. Concluding remarks

In this paper we have shown that in favourable situations we can use the sample size to modify the kinetic regime of the overall transformation. A slowing down is expected at small sizes. Accordingly, this provides a possibility of expanding the apparent domian of metastability. Only a kinetic effect may occur independently of the well-known Gibbs–Thomson effect. From the changes in the isothermal kinetics, we can thus separately estimate the values of the nucleation and growth rates at the studied temperature.

The knowledge of $N$ at one temperature can be used instead of the surface free energy to estimate $N(T)$ in the framework of the classical homogeneous capillarity theory. Application to the ordering transformation of a glassy crystal has allowed the maximum of $N(T)$ to be located somewhat above $T_g$. It is interesting to note that this maximum does exist, whereas the critical radius is found to be $r^* \sim 15$ Å, only slightly greater than the unit cell size corresponding to phase III (see inset of Fig. 7). This may explain why phase IV, which is expected to have a more simple crystal structure, is the first product of the transformation under deep super-cooling.

The second point discussed in this paper is the transient nature of this metastable phase IV which is revealed when the initial transformation I → IV has occurred during an annealing near the glass transition temperature. Upon reheating we observe a reversion of the order which occurs at temperatures well below the expected transition temperature $T_{IV-I}$. These reversion temperatures are found to closely depend on the annealing conditions and we have established that they are correlated to the cluster size of phase IV. The exact origin of the extraordinary phenomenon by which a system can go back to a metastable state once it has escaped from the latter is, however, not yet understood. It will be important to determine if this (apparently) size-induced transformation is the result of a kinetic or thermodynamic process.

## Acknowledgements

This work was performed in the framework of an EEC (FEDER) collaboration program between Nord Pas de Calais (F) and Kent (GB).

## References

[1] K. Adachi, H. Suga and S. Seki, Bull. Chem. Soc. Jpn., 41 (1986) 1073.
[2] H. Suga, Ann. N.Y. Acad. Sci., 484 (1986) 248.
[3] J.N. Sherwood (Ed), The Plastically Crystalline State, Wiley, New York, 1979.
[4] H. Suga, J. Chem. Thermodyn., 25 (1993) 463.
M. Descamps, J.F. Willart and O. Delcourt, Physica A, 201 (1993) 346.

[5] J.F. Willart, M. Descamps, M. Bertault and N. Benzakour, J. Phys. C, Condensed Matter, 4 (1992) 9509.
[6] J.F. Willart, M. Descamps and N. Benzakour, J. Chem. Phys., in press.
[7] M. Descamps, J.F. Willart, G. Odou and K. Eichhorn, J. Phys. I, 6 (1992) 813.
[8] O. Delcourt, M. Descamps and H. Hillorst, Ferroelectrics, 124 (1991) 109.
[9] R. Becker and W. Döring, Ann. Phys., 24 (1935) 719.
D. Turnbull and J.C. Fisher, J. Chem. Phys., 17 (1949) 71.
D.W. Oxtoby, Ann. N.Y. Acad. Sci., 484 (1986) 26.
[10] D. Turnbull, Solid State Phys., 3 (1956).
[11] N. Yamamia, Y. Yamada, J.D. Axe, D.P. Belanger and S.M. Shapiro, Phys. Rev. B, 33 (1986) 7770.
[12] J.P. Amoureux, G. Noyel, M. Foulon, M. Bee and M. Jorat, Molec. Phys., 52 (1984) 161.
[13] C.T. Moynihan, P.B. Macedo, C.J. Montrose, P.K. Gupta, M.A. Debolt, J.F. Dill, B.E. Dom, P.W. Drake, A.J. Easteal, P.B. Elterman, R.P. Moeller, H. Sasabe and J.A. Wilder, Ann. N.Y. Acad. Sci., 279 (1976) 15.